



Li, T., Wang, Z., Chen, W., Miras, H. N., and Song, Y.-F. (2017) Rational design of a polyoxometalate intercalated layered double hydroxide: highly efficient catalytic epoxidation of allylic alcohols under mild and solvent-free conditions. *Chemistry: A European Journal*, 23(5), pp. 1069-1077.

There may be differences between this version and the published version. You are advised to consult the publisher's version if you wish to cite from it.

<http://eprints.gla.ac.uk/133859/>

Deposited on: 25 January 2017

Enlighten – Research publications by members of the University of Glasgow
<http://eprints.gla.ac.uk>

Rational Design of a Polyoxometalate Intercalated Layered Double Hydroxides: Highly Efficient Catalytic Epoxidation of Allylic Alcohols Under Mild and Solvent-free Conditions

^aState Key Laboratory of Chemical Resource Engineering, Beijing University of Chemical Technology, 100029 Beijing, China. Email: songyufei@hotmail.com or songyf@mail.buct.edu.cn;

^bWestCHEM, School of Chemistry, University of Glasgow, University Avenue, Glasgow, G12 8QQ, UK. E-mail: charalampos.moiras@glasgow.ac.uk

Abstract: Intercalation catalysts, owing to the modular and accessible gallery and unique inter-lamellar chemical environment, have shown wide application in various catalytic reactions. However, the poor mass transfer between the active components of the intercalated catalysts and organic substrates is one of the challenges that limit their further application. Herein, we fabricate a novel heterogeneous catalyst by intercalating the polyoxometalate (POM) of Na₉LaW₁₀O₃₆·32H₂O (LaW₁₀) into layered double hydroxides (LDHs), which has been covalently modified with ionic liquids (ILs). The intercalation catalyst demonstrates high activity and selectivity for epoxidation of various allylic alcohols in the presence of H₂O₂. Taking trans-2-hexen-1-ol as an example, it shows up to 96 % conversion and 99 % epoxide selectivity at 25 °C in 2.5 h. To the best of our knowledge, the Mg₃Al-ILs-C8-LaW₁₀ composite material constitutes one of the most efficient heterogeneous catalysts for epoxidation of allylic alcohols (including the hydrophobic allylic alcohols with long alkyl chains) reported so far.

Keywords: Layered double hydroxides, Polyoxometalates, Epoxidation, Ionic liquid, Allylic alcohol

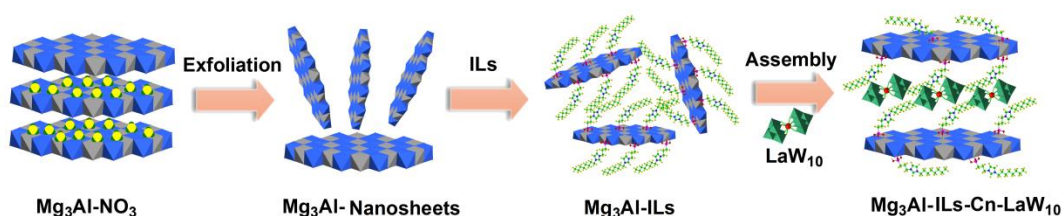
Introduction

Epoxidation of allylic alcohols is of great importance [1-5] since the resultant epoxides are widely utilized as raw materials for epoxy resins and as building blocks for synthesis of fine chemicals and biologically important pharmaceuticals [6-8]. The application of epoxides is growing rapidly every year in chemical industry, giving rise to remarkable attentions in scientific community and industry. To date, a large number of catalysts have been investigated for epoxidation, in which polyoxometalates (POMs), such as $[\text{WZnM}_2(\text{ZnW}_9\text{O}_{34})_2]^{n-}$ [M=Mn(II), Ru(III), Fe-(III), Pd(II), Pt(II), Zn(II); n=10-12] [9], $[\gamma\text{-PW}_{10}\text{O}_{38}\text{V}_2(\mu\text{-OH})_2]^{3-}$ [10], $[\text{PMo}_{11}\text{Mn}(\text{H}_2\text{O})\text{O}_{39}]^{5-}$ [11] etc, have shown to be efficient for epoxidation reactions. However, the common issues associated with the homogeneous catalysts, such as the easy agglomeration and difficulty during the recycling process largely restrict their application. The urgency of environmentally-benign and sustainable approaches to chemical processes stimulates the requirement for recyclable heterogeneous catalyst as alternative to unfavorable homogeneous catalyst. Under such circumstances, some heterogeneous catalysts including Mo-AMP-CuBTC (AMP = 4-aminopyridine; BTC = benzene-1,3,5-tricarboxylate) [12], vanadium-based complexes [13] and Co-MCM-41 [14], were developed and applied for epoxidation of allylic alcohols. For these heterogeneous catalytic systems reported so far, 1) toxic organic solvents or additives such as toluene, dichloromethane *etc* were used [13,15], which are generally highly corrosive and carcinogenic, and require frequent and laborious work-up treatments; 2) the accessibility of the substrates and the active components was limited [16]; 3) these systems exhibit quite often catalyst leaching and thermal stability issues, thus no scale-up experiments were carried out [17]. Consequently, it is of great significance to develop efficient, recyclable, and environmentally-benign heterogeneous catalytic systems for epoxidation of allylic alcohols.

Ionic liquids (ILs) can be used as novel green solvents or advanced catalytic materials, which are receiving keen interest currently due to their unique properties such as intramolecular forces, ionicity, polarity, and their inherent nature [18]. As a result, research involving ILs is expanding to many different areas of knowledge [1,19,20]. Layered double hydroxides (LDHs) or hydrotalcite-like compounds are a large family of two-dimensional (2D) anionic clay materials which can be represented by the general formula $[\text{M}_{1-x}^{2+}\text{M}_x^{3+}(\text{OH})_2]^{x+}[\text{A}_{x/n}]^{n-} \cdot m\text{H}_2\text{O}$ [21,22]. The 2D inorganic

matrix of LDHs consist of brucite-like host sheets with edge-sharing octahedra and the lateral particle sizes range from nanometer to micrometer scale.

On the basis of previous reports, it can be summarized that an efficient heterogeneous catalytic system for epoxidation should take into consideration of the following aspects: a) green solvents or solvents-free medium should be applied; b) close proximity of the substrates and the active species; c) structural stability of the catalytic system. Bearing these in mind, we report the design and fabrication of a novel heterogeneous catalyst by intercalation of $\text{Na}_9\text{LaW}_{10}\text{O}_{36}\cdot 32\text{H}_2\text{O}$ (LaW_{10}) into ionic liquids (ILs) modified LDHs. The intercalation catalyst shows highly efficient epoxidation of various allylic alcohols in the presence of H_2O_2 at 25 °C under organic solvent-free conditions.



Scheme 1. Schematic illustration of the synthetic procedure for the catalysts $\text{Mg}_3\text{Al-ILs-Cn-LaW}_{10}$ ($n=4, 8, 12$).

Results and Discussion

Preparation and characterization of $\text{Mg}_3\text{Al-ILs-Cn-LaW}_{10}$. $\text{Mg}_3\text{Al-ILs-Cn-LaW}_{10}$ ($n = 4, 8, 12$) were prepared according to the procedures illustrated in Scheme 1. First, the $\text{Mg}_3\text{Al-NO}_3$ was exfoliated into LDH-nanosheets in formamide solution. Next, the $(\text{EtO})_3\text{Si-ILs-Cn}$ ($n = 4, 8, 12$) was covalently anchored onto the LDHs layers *via* condensation reaction. Further on, the $\text{Mg}_3\text{Al-ILs-Cn-LaW}_{10}$ was obtained by adding LaW_{10} into the above mixture. Such exfoliation and assembly strategy has been applied successfully in a number of POMs/LDHs composites.[25]

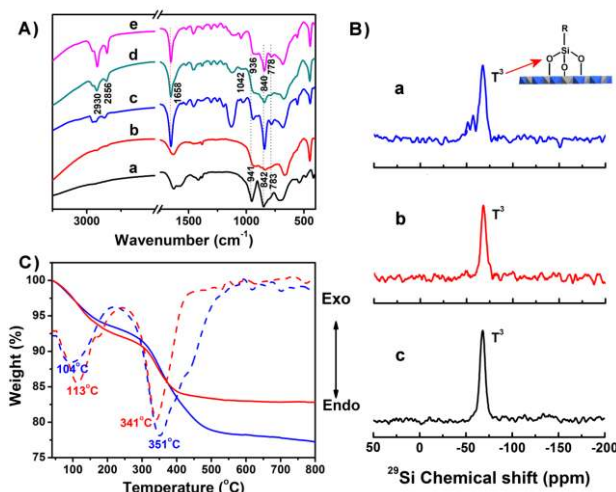


Figure 1. A) FT-IR spectra of (a) Na₉LaW₁₀O₃₆·32H₂O; (b) Mg₃Al-LDW₁₀; (c) Mg₃Al-ILs-C4-LDW₁₀; (d) Mg₃Al-ILs-C8-LDW₁₀; (e) Mg₃Al-ILs-C12-LDW₁₀; B) Solid-state ²⁹Si CP/MAS NMR spectra of (a) Mg₃Al-ILs-C4-LDW₁₀; (b) Mg₃Al-ILs-C8-LDW₁₀; (c) Mg₃Al-ILs-C12-LDW₁₀; inset picture shows the structure model of T³; C) TG-DTA profile of Mg₃Al-LDW₁₀ (red) and Mg₃Al-ILs-C8-LDW₁₀ (blue).

As shown in Figure 1A, FT-IR spectrum of LaW10 exhibits characteristic peaks at 941, 842 and 783 cm⁻¹, which can be attributed to the vibrations of W-O_t, W-O_c-W and W-O_e-W (t, terminal; c, corner-sharing; e, edge-sharing),[26] respectively. These W-O stretching bands can be clearly observed in the FTIR spectra of Mg₃Al-LDW₁₀ and Mg₃Al-ILs-C_n-LDW₁₀ (n = 4, 8, 12). Taking Mg₃Al-ILs-C8-LDW₁₀ as an example, its W-O stretching bands with slight shifts to 936, 840 and 778 cm⁻¹, respectively, due to the interactions between host layers and guest anions. FT-IR spectrum of Mg₃Al-ILs-C_n-LDW₁₀ (n = 4, 8, 12) also exhibits newly-appeared C-H stretching vibrations at 2930 and 2856 cm⁻¹ due to the alkyl chain -CH₂ and -CH₃, and the C=N stretching at 1658 cm⁻¹ because of the imidazole of ILs, respectively. Additionally, the bands in the 1030-1045 cm⁻¹ region are observed in the Mg₃Al-ILs-C_n-LDW₁₀ (n = 4, 8, 12) samples, which are assigned to the vibration of Si-O-M bond (M = Al, Mg).[27] It should be noted that FT-IR spectrum of Mg₃Al-NO₃ shows stretching bands at 1384 cm⁻¹ is assigned to the N-O vibration of NO₃⁻ (Figure S1),[28] which disappears in the corresponding FT-IR spectra of Mg₃Al-LDW₁₀ and Mg₃Al-ILs-C_n-LDW₁₀ (n = 4, 8, 12), indicating the complete exchange of NO₃⁻ by the LaW10. All these facts demonstrate that the ILs have been grafted onto the layers of LDHs and the guest anions LaW10 have been intercalated into LHDs successfully. FT-IR spectra of (EtO)₃Si-ILs-C_n (n=4, 8, 12) are shown in Figure S2. As shown in Figure 1B, the solid-state ²⁹Si cross-polarization magic-angle

spinning (CP/MAS) NMR spectra of Mg₃Al-ILs-Cn- LaW10 (n = 4, 8, 12) samples exhibit resonance peaks centered at -66.4 ppm (Mg₃Al-ILs-C4-LaW10), -66.7 ppm (Mg₃Al-ILs-C8-LaW10) and -67.0 ppm (Mg₃Al-ILs-C12-LaW10), respectively, which correspond to T3 [Si(OM)₃],[29] The presence of T3 signal indicates there are three M-O-Si bonds around the Si atom. These results confirm that the ILs are tethered onto the layers of LDHs covalently, resulting in the formation of Mg-O-Si and/or Al- O-Si in LDHs layers.

Thermogravimetry with differential thermal analysis (TGDTA) of Mg₃Al-LaW10 and Mg₃Al-ILs-Cn-LaW10 (n = 4, 8, 12) have been carried out in order to investigate the thermal stabilities. As shown in Figure 1C, the TG-DTA of Mg₃Al-LaW10 shown for comparison, exhibits a two-stage weight loss. The first one take place in the range of 25 to 230 oC and is due to the loss of water molecules adsorbed on the surface and interlayer space, whereas the second weight loss can be attributed to the structural compromise of the layered structure of LDHs. Similarly, in the case of Mg₃Al-ILs-C8-LaW10, two main weight-loss stages can be observed, where the first weight loss of 6.58 % between 25 and 220 oC can be ascribed to the removal of water molecules absorbed on the surface and interlayer, and the second weight loss of 16.15 % between 220 and 650 oC corresponds to the collapse of the layered structure and decomposition of the ionic liquid. The thermal stabilities of Mg₃Al-ILs-C4-LaW10 and Mg₃Al-ILs-C12-LaW10 are similar to that of Mg₃Al-ILs-C8-LaW10 (Figure S3). Based on the TG-DTA and elemental analysis results, the composition of Mg₃Al-ILs-Cn- LaW10 can be determined (Table S1). For example, the composite material of Mg₃Al-ILs-C8-LaW10 can be identified as Mg_{0.75}Al_{0.25}(OH)_{1.88}[O₃SiC₁₄H₂₈N₂]_{0.04}[PF₆]_{0.011} [LaW10O₃₆]_{0.031} · 0.58H₂O; (Mg=11.26 wt. %, Al=4.22 wt. %, W=35.67 wt. %, ILs=7.51 wt. %, LaW10=193.85 μmol/g).

XRD data of Mg₃Al-CO₃ and Mg₃Al-NO₃ revealed basal spacing of 0.76 nm, 0.89 nm, respectively. For Mg₃Al-ILs-C8- LaW10, the calculated gallery height value of 1.02 nm was determined by subtracting the thickness of the host layer (0.48 m) from the value of the *d*(003) spacing (Table S1),[30] which are in good agreement with the diameter of the short axis of the LaW10 cluster.[31] This observation suggests that the LaW10 clusters are intercalated with the short axis perpendicular to the layers of LDHs.

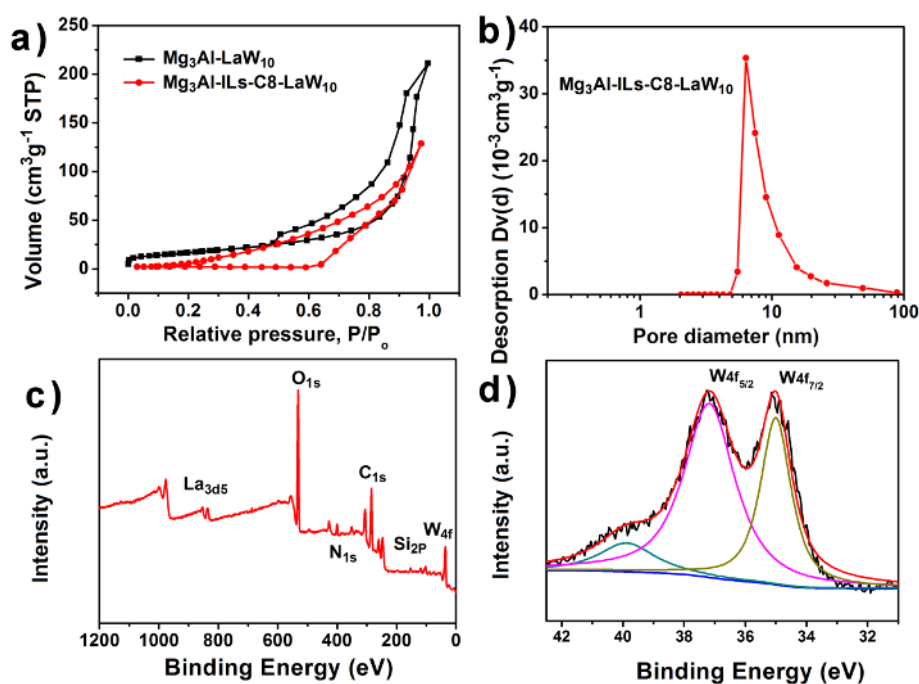


Figure 2. a) The N₂ adsorption-desorption isotherms of Mg₃Al-LaW₁₀ and Mg₃Al-ILs-C8-LaW₁₀; b) the pore diameter distribution of Mg₃Al-ILs-C8-LaW₁₀; c) XPS survey spectrum of Mg₃Al-ILs-C8-LaW₁₀; d) XPS spectrum for the W4f core level of Mg₃Al-ILs-C8-LaW₁₀ sample.

As shown in Figure 2a, the Mg₃Al-LaW₁₀ and Mg₃Al-ILs-C8-LaW₁₀ exhibit a type I adsorption isotherm at relative lower pressure ($P/P_0 < 0.1$), and a H3 type N₂ hysteresis loop at relative higher pressure ($P/P_0 > 0.6$) according to BDDT (Brunauer, Deming, Deming and Teller) classification, indicating the presence of both interlayer micropores and inter-particle mesopores. Furthermore, the surface areas of Mg₃Al-LaW₁₀ and Mg₃Al-IL-C8-LaW₁₀ are 59.56 and 63.16 m²/g (Table S1), respectively. The pore diameter distribution of Mg₃Al-ILs-C8-LaW₁₀ is calculated by the Barret-Joyner-Halenda (BJH) method showed a peak centered at around 5.87 nm (Figure 2b).

The X-ray photoelectron spectroscopy (XPS) was used to characterize the Mg₃Al-ILs-C8-LaW₁₀ composite material. As shown in Figure 2c, the photoelectron peaks of C, O, N, Si, La and W *et al* elements can be clearly observed. Moreover, the W(4f) photoemission peak can also be observed (Figure 2d), which consists of two peaks originating from the spin orbital splitting of the 4f_{7/2} and 4f_{5/2} located at 35.2 eV and 37.3 eV, respectively. The doublets are ascribed to the W in the W-O bond configuration and are observed typically for W⁶⁺. [32] This result is in accordance with the oxidation state of W of LaW₁₀. The oxidation state of the tungsten centers in the

composites Mg₃Al-ILs-C4-LaW₁₀ (Figure S4) and Mg₃Al-ILs-C12-LaW₁₀ (Figure S5) are also in agreement with the oxidation states of the starting material (LaW₁₀).

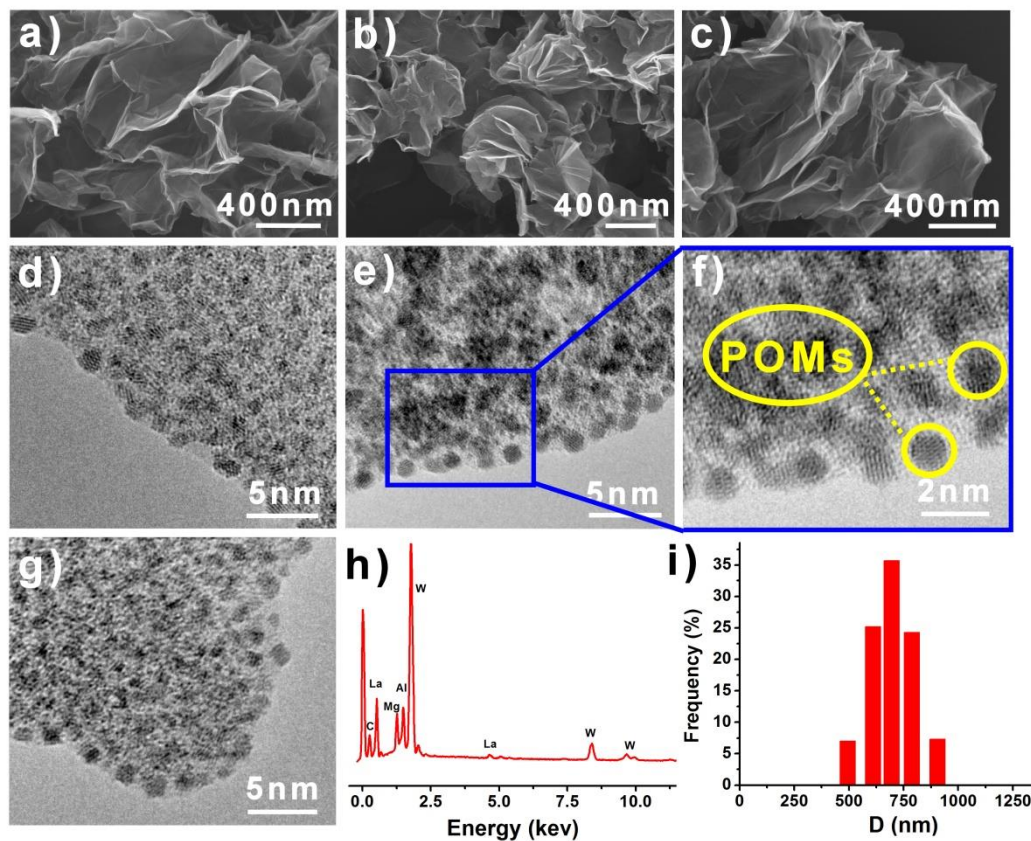


Figure 3. SEM images of a) Mg₃Al-ILs-C4-LaW₁₀; b) Mg₃Al-ILs-C8-LaW₁₀; c) Mg₃Al-ILs-C12-LaW₁₀; HRTEM images of d) Mg₃Al-ILs-C4-LaW₁₀; e-f) Mg₃Al-ILs-C8-LaW₁₀; g) Mg₃Al-ILs-C12-LaW₁₀; h) EDS of Mg₃Al-ILs-C8-LaW₁₀; i) size distributions of Mg₃Al-ILs-C8-LaW₁₀.

SEM images of the Mg₃Al-ILs-C_n-LaW₁₀ (n=4, 8, 12) samples (Figure 3a-c) show the porous stacking of sheet-like crystallites. Taking Mg₃Al-ILs-C8-LaW₁₀ as an example, we can see clearly the particle sizes of these crystallites are ~700 nm. Figure 3d-g illustrates the HRTEM images of the Mg₃Al-ILs-C_n-LaW₁₀ (n=4, 8, 12) samples. The black spots of 1~1.5 nm (denoted by yellow circle in Figure 3f) in diameter are highly dispersed. From the partial enlarged areas in figure 3f, the size of the black spots is in good agreement with the size of LaW₁₀ clusters, and these results further suggest that the LaW₁₀ anions are incorporated into the interlayer of LDHs successfully. Energy-dispersive X-ray spectrometry image of Mg₃Al-ILs-C8-LaW₁₀ (Figure 3h) demonstrates the presence of C, La, Mg, Al, and W *et al* elements, which is in a good consistent with the structure and composition of Mg₃Al-ILs-C8-LaW₁₀. Dynamic light scattering (DLS) measurement of

Mg₃Al-ILs-C8-LaW₁₀ shows that the particle size is narrowly distributed with the average diameter of ~700 nm (Figure 3i).

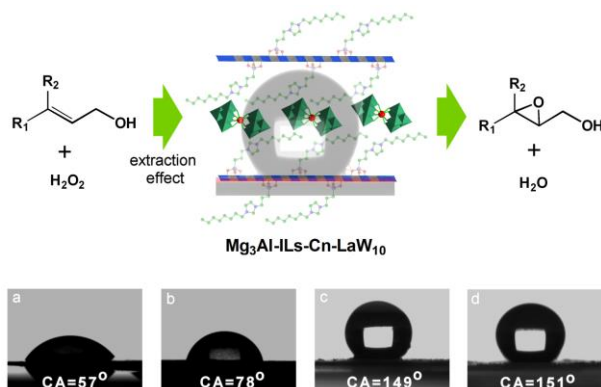
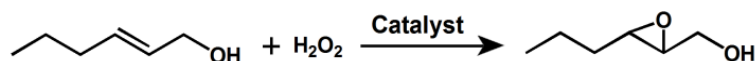


Figure 4. Schematic diagram of the catalytic process (top); the water contact angle measurements of (a) Mg₃Al-LaW₁₀; (b) Mg₃Al-ILs-C4-LaW₁₀; (c) Mg₃Al-ILs-C8-LaW₁₀; (d) Mg₃Al-ILs-C12-LaW₁₀, respectively.

To illustrate the interaction between the catalyst and the allylic alcohols under the experimental conditions, the amphiphilic properties of the catalysts were investigated. As shown in Figure 4c, the contact angle of approximately 149° indicates that the Mg₃Al-ILs-C8-LaW₁₀ is highly hydrophobic. In the case of Mg₃Al-ILs-C12-LaW₁₀, upon increase of the alkyl chain length, it shows an increase of the contact angle to a value of 151°. In contrast, the contact angles of Mg₃Al-LaW₁₀ and Mg₃Al-ILs-C4-LaW₁₀ are 57° and 78°, respectively (Figure 4a-d). These results suggest that after ILs modification of the LDHs layers, the hydrophobicity increases according to the following sequence Mg₃Al-ILs-C4-LaW₁₀ < Mg₃Al-ILs-C8-LaW₁₀ ≈ Mg₃Al-ILs-C12-LaW₁₀, ensuring readily access of the substrate to the catalytic site due to the hydrophobic-hydrophobic interactions.



Scheme 2. Model reaction of the epoxidation of allylic alcohols.

Table 1. Solvent-free epoxidation of *trans*-2-hexen-1-ol with different catalysts.^[a]

Entry	Catalyst	Conversion ^[b] (%)	Selectivity ^[b] (%)
1	None	0	-

2	Mg ₃ Al-LaW ₁₀	47.0	99
3	Mg ₃ Al-ILs-C4-LaW ₁₀	87.0	99
4	Mg ₃ Al-ILs-C8-LaW ₁₀	95.4	99
5	Mg ₃ Al-ILs-C12-LaW ₁₀	79.0	99

[a] Reaction conditions: 2 mmol of *trans*-2-hexen-1-ol, 2.4 mmol of H₂O₂ (30 wt.%), 20 mg of the catalyst, T = 25 °C, t = 2.5 h; [b] Conversion and selectivity were determined by GC analysis using reference standards. Assignment of *trans*-2-hexen-1-ol epoxide was analysed by ¹H NMR and ¹³C NMR in **Figure S6**.

Optimization of catalyst. As shown in Table 1, taking epoxidation of *trans*-2-hexen-1-ol as an example, the reaction hardly takes place without catalyst (entry 1). The catalyst of Mg₃Al-LaW₁₀ exhibits only 47 % conversion at 25 °C, 2.5 h (entry 2). In contrast, the intercalated catalysts of Mg₃Al-ILs-C_n-LaW₁₀, (n = 4, 8, 12) demonstrate better catalytic activity than Mg₃Al-LaW₁₀ (entry 3-5). Notably, the Mg₃Al-ILs-C8-LaW₁₀ exhibits better catalytic performance with 96.0 % conversion and 99 % selectivity (entry 4) under the same experimental conditions.

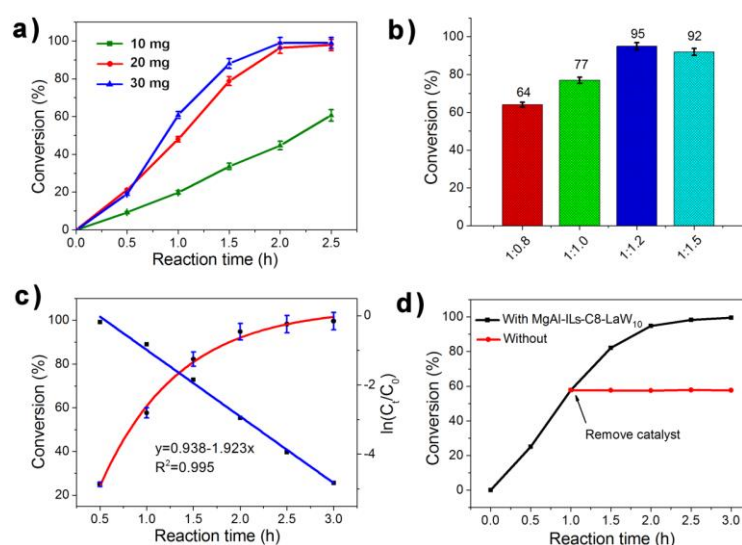


Figure 5. a) Effect of Mg₃Al-ILs-C8-LaW₁₀ amount on catalytic epoxidation of *trans*-2-hexen-1-ol (The data were obtained by carrying out parallel experiments under the same experimental conditions). B) Effect of Substrate/H₂O₂ molar ratio on catalytic epoxidation of allylic alcohols. Reaction conditions: 2 mmol *trans*-2-hexen-1-ol, 20 mg Mg₃Al-ILs-C8-LaW₁₀, T = 25 °C, 2.5 h; c) Kinetic profiles of epoxidation in scale-up experiment; Reaction conditions: 20 mmol *trans*-2-hexen-1-ol, 24 mmol H₂O₂ (30 wt. %), 200 mg Mg₃Al-ILs-C8-LaW₁₀, T = 25 °C. d) Experiment to prove the nature of heterogeneous catalyst Mg₃Al-ILs-C8-LaW₁₀.

Effect of catalyst dosage. On the basis of the results reported in Table 1, we selected the Mg₃Al-ILs-C8-LaW₁₀ for further investigation of the epoxidation reaction of allylic alcohols. The influence of the amount of the catalyst on the epoxidation of allylic alcohols was studied by varying the catalyst dosage from 10 mg to 30 mg while maintaining the H₂O₂/substrate molar ratio constant (2.4 mmol H₂O₂; 2 mmol substrate). Figure 5a illustrates the epoxidation of *trans*-2-hexen-1-ol as a function of time at different catalyst dosage. With the increase of the catalyst dosage from 10, 20 to 30 mg, the conversion of *trans*-2-hexen-1-ol increases from 60 %, 96 % to 97 % accordingly, respectively, at 25 °C in 2.5h. Therefore, 20 mg of Mg₃Al-ILs-C8-LaW₁₀ will be applied for the following studies.

Effect of the substrate/H₂O₂ molar ratio. As shown in Figure 5b, with the molar ratio of substrate/H₂O₂ varies from 1:0.8, 1:1.0, 1:1.2 to 1:1.5, the conversion of epoxidation of *trans*-2-hexen-1-ol changes from 64 %, 77 %, 95.4 % to 92.0 %, respectively. Therefore, the epoxidation reaction has been performed using the initial molar ratio of substrate/H₂O₂ at 1:1.2 under solvent-free condition.

Effect of solvents. Investigation of solvents effect on the epoxidation of *trans*-2-hexen-1-ol using Mg₃Al-ILs-C8-LaW₁₀ shows that the conversion of 18.37 %, 19.72 %, 21.96 % and 10.82 % in methanol, ethanol, acetonitrile and ethyl acetate, respectively, can be obtained (Figure S7).-Notably, the direct mixing of *trans*-2-hexen-1-ol with Mg₃Al-ILs-C8-LaW₁₀ without solvent shows remarkable conversion of allylic alcohols to the corresponding epoxides. We assume that the presence of ILs anchored on the layers promotes the interactions between the catalyst and substrate, leading to the increase of catalytic efficiency. Note that the epoxidation reactions have been performed on solvent-free condition.

Kinetic study of epoxidation of allylic alcohol. To obtain the kinetic parameters for epoxidation of allylic alcohols, a scaled-up experiment was performed with 20 mmol *trans*-2-hexen-1-ol, 24 mmol of H₂O₂ (30 wt. %) and 200 mg catalyst Mg₃Al-ILs-C8- LaW₁₀ at 25 oC under solvent-free conditions. Conversion and $\ln(Ct/C0)$ are plotted against reaction time in Figure 5c, in which $C0$ and Ct are initial allylic alcohols concentration and allylic alcohols concentration at time t , respectively. The Mg₃Al-ILs-C8- LaW₁₀ shows excellent catalytic activity and the conversion can reach 94.76 % in 2 hours. The linear fit of the data reveals that the catalytic reaction exhibits pseudo-first-order kinetics for the epoxidation of allylic alcohols reaction ($R^2= 0.995$). The rate constant k for epoxidation reaction was determined to be 1.923 h⁻¹ on the basis of Eqs. (1) and (2). Epoxidation

of *trans*-2-hexen-1-ol could be completed with the conversion of 98.24 % in 2.5 h and 99.2 % in 3 h. Thus, the Mg3Al-ILs-C8-LaW10 exhibits high catalytic efficiency for epoxidation of allylic alcohols, and the catalytic reaction strictly obey pseudo-first-order kinetics with > 99 % selectivity of corresponding epoxides. In order to compare the kinetic parameters with different intercalation catalysts for epoxidation of allylic alcohols, we also investigate the kinetic parameters of Mg3Al-LaW10, Mg3Al-ILs-C4-LaW10 and Mg3Al-ILs-C12-LaW10 (Figure S8).

$$\frac{-dC_t}{dt} = kC_t \quad (1)$$

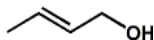
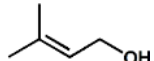

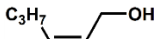
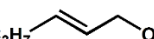
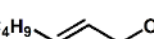
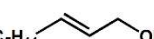
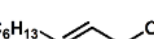

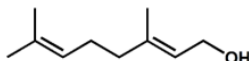
$$\ln \left[\frac{C_t}{C_0} \right] = -kt \quad (2)$$

To confirm that the catalyst of Mg3Al-ILs-C8-LaW10 is a truly heterogeneous catalyst, the epoxidation reaction of allylic alcohol was carried out using Mg3Al-ILs-C8-LaW10 as the catalyst and H₂O₂ as the oxidant at 25 °C under solvent-free conditions. When the conversion reaches about 55 % in 1 h, the solid catalyst can be filtered by simple filtration. The reaction mixture is allowed to proceed under the same experimental conditions. It was observed that no additional *trans*-2-hexen-1-ol can be transformed into the corresponding epoxides (Figure 5d). While the solid catalyst Mg3Al-ILs-C8-LaW10 is added back to the reaction mixture, the catalytic reaction continued at the expected rate. This result suggests that Mg3Al-ILs-C8-LaW10 is a true heterogeneous catalyst. To demonstrate the wide applicability of the catalytic system, epoxidation of various allylic alcohols were carried out at 25 °C under solvent-free conditions. As shown in Table 2, the Mg3Al-ILs-C8-LaW10 exhibits excellent epoxidation results for different substrates. For example, epoxidation of 2-buten-1-ol, 3-methyl-2-buten-1-ol, *cis*-2-penten-1-ol results in 92 %, 99 %, and 93 % conversion and TOF values of 587, 1010, 475 h⁻¹, respectively (entry 1-3). In contrast, the Mg3Al-LaW10 shows only 78 %, 75 % and 57 % conversion for the above-mentioned substrates. These values can be explained based on size considerations of the substrates and their accessibility to the active species in the restricted region of LDHs.

Upon increase of the length and hydrophobicity of the alkyl chains, the difference of the catalytic efficiency becomes more pronounced in the case of Mg3Al-LaW10 and Mg3Al-ILs-C8-LaW10. In the case of *cis*-2-hexen-1-ol and *trans*-2-hexen-1-ol, the obtained conversion values found to be

93 % and 96 % using Mg₃Al-ILs-C8-LaW10 as catalyst with the selectivity of 99 % (entry 4-5), respectively, whereas in the Mg₃Al-LaW10 composite, exhibited 72 % and 45 %, respectively. It is worth noting that a few heterogeneous catalysts demonstrated great epoxidation activity for long hydrophobic allylic alcohols. Using, *trans*-2-hepten-1-ol, *trans*-2-octen-1-ol, *trans*-2-nonen-1-ol, *cis*-2-nonen-1-ol and geraniol as substrates, the Mg₃Al-ILs-C8-LaW10 exhibited excellent catalytic performance with upon increase of the reaction temperature to 50 oC (entry 6-10). Interestingly, the highly efficient epoxidation results for geraniol is due to the fact that the oxygen transfer takes place to the proximal 2,3-allylic double bond rather than to the remote 6,7- double bond, leading to the regioselective epoxidation of geraniol.[2,10,33] In contrast, Mg₃Al-LaW10 exhibited much lower conversion due to the poor mass transfer ability in the absence of the grafted ionic liquids. The catalytic activity for epoxidation of various allylic alcohols using Mg₃Al-ILs-C4-LaW10 and g₃Al-ILs-C12-LaW10 are listed in Table S2-3.

Table 2. Epoxidation of various allylic alcohols using Mg₃Al-LaW₁₀ and Mg₃Al-ILs-C8-LaW₁₀ as catalyst in the presence of H₂O₂.

Entry	Substrate	T (°C)	Time (h)	Mg ₃ Al-LaW ₁₀		Mg ₃ Al-ILs-C8-LaW ₁₀		
				Conv (%)	Selec (%)	Conv (%)	Selec (%)	TOF (h ⁻¹)
1		25	0.8	78	99	92	99	58/7
2		25	0.5	75	99	99	99	1010
3		25	1.0	57	99	93	99	475
4		25	2.5	72	99	93	99	190
5		25	2.5	45	99	96	99	196
6		50	3.0	50	97	94	97	157
7		50	3.0	18	96	85	96	140
8		50	3.0	6	95	82	95	134
9		50	3.0	8	98	88	98	148
10		50	2.0	31	93	92	93	220

Note: Reaction conditions: 2 mmol substrate, 2.4 mmol H₂O₂, 20 mg catalyst; Conversion and selectivity were determined by GC analysis using reference standards; TOF = moles of product/(moles of catalyst used × reaction time).

Comparison with other reported heterogeneous catalyst: Catalytic epoxidation of *trans*-2-hexen-1-ol using different heterogeneous catalysts reported in the literature are summarized in Table 3. The epoxidation of *trans*-2-hexen-1-ol using Mg₃Al-ILs-C8-LaW₁₀ as catalyst exhibits two prominent features including 1) solvent-free condition and 2) excellent epoxidation conversion (96 %) and selectivity (99 %) have been obtained at 2.5 h at 25 oC under environmentally-benign conditions. In contrast, other heterogeneous catalysts either use CH₃CN, toluene or CH₂Cl₂ solvents (entry 1-11), or exhibit inferior catalytic activity. For example, the [PO₄{WO(O₂)₂}₄]-PIILP, took much longer reaction time of 4.0 h in CH₃CN in order to reach a comparable performance (entry 9); For KW₂O₃(O₂)₄(H₂O)₂, longer reaction time was applied (5 h) in order to get good catalytic result (entry 12, homogeneous system).

Table 3. Catalytic epoxidation of *trans*-2-hexen-1-ol using different heterogeneous catalysts.

Entry	Catalyst	t (h)	T (°C)	Sub/oxidant ^a molar ratio	Solvent	Conv. (%)	Selec. (%)	Ref
1	Mg ₃ Al-WZn ₃ (ZnW ₉ O ₃₄) ₂	1.0	50	1:2	CH ₃ CN	80	99	34
2	MNP ₁₁ -Si-inic-Mo	24.0	80	1:2 ^b	Toluene	88	96	17
3	MCM-Pr-1	24.0	55	1:2 ^b	CH ₂ Cl ₂	75	100	16
4	Fe ₃ O ₄ @SiO ₂ @APTMS@V-MIL-101	24.0	80	1:1.2 ^b	CH ₃ CN	100	100	35
5	WO ₂ (acac) ₂	3.0	RT	1 : 2	CH ₂ Cl ₂	92	95	36
6	(TBA) ₂ [SeO ₄ {WO(O ₂) ₂ } ₂]	3.0	32	1:1	CH ₃ CN	89	-	18
7	SiO ₂ @2-Peracaroxyethyl	2.0	RT	1:2 ^c	CH ₂ Cl ₂	99	99	37
8	VO(acac) ₂ -BBHA	5.0	0	1:3 ^b	Toluene	75	80	14
9	[PO ₄ {WO(O ₂) ₂ } ₄]-PIILP	4.0	50	1:2	CH ₃ CN	99	94	38
10	MS _n -bpy-Mo ^{VI}	24.0	55	1:1.2 ^b	CH ₂ Cl ₂	30	71	39
11	[ZnWZn ₂ (H ₂ O) ₂ (ZnW ₉ O ₃₄) ₂]	4.0	21	1:2	CH ₃ CN	100	99	40
12	K-W ₂ O ₃ (O ₂) ₄ (H ₂ O) ₂]	5	32	1:1	H ₂ O	98	100	41
13	MgAl-WZn ₃ (ZnW ₉ O ₃₄) ₂	2.5	50	1:1.2	None	90	99	42
14	IL-Nb ₂ O ₇	8.0	0	1:1.2	None	62.4	99	43
15	[TBA][Nb=O(O-O)(OH) ₂]	12.0	0	1:1	None	85	99	1
16	Mg ₃ Al-ILs-C8-LaW ₁₀	2.5	25	1:1.2	None	96	99	This work

Note: a. Unless specified, the oxidant is H₂O₂ in most case; b. TBPH as oxidants; c. peracid as oxidants.

For MgAl-WZn₃(ZnW₉O₃₄)₂, higher temperature was applied (50oC) in order to achieve good catalytic results (entry 13); In the case of IL-Nb₂O₇ (entry 14) and [TBA][Nb=O(O-O)(OH)₂] (entry 15), long reaction time 8.0 h and 12.0 h were used, resulting in 62.4 % and 85 % conversion,

respectively, under solvent free conditions. To the best of our knowledge, Mg₃Al-ILs-C8-LaW₁₀ is one of the most efficient heterogeneous catalysts for epoxidation of allylic alcohols.

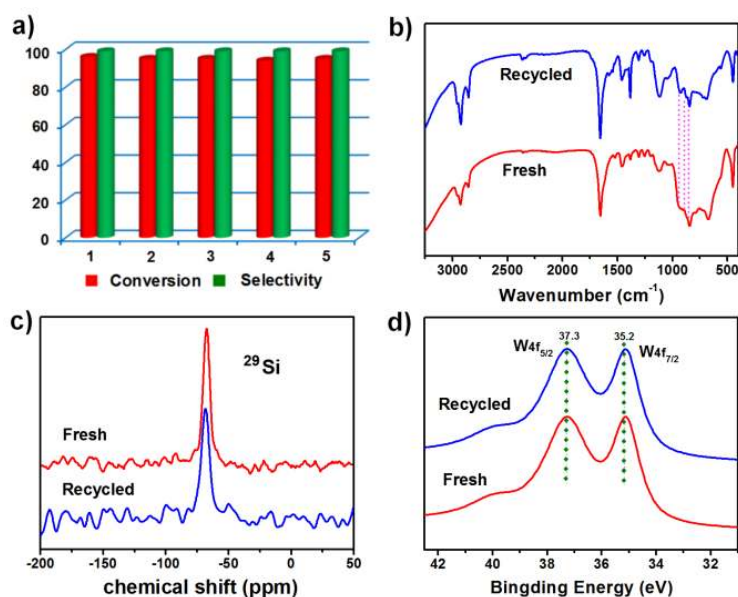


Figure 6. a) Recycling of the Mg₃Al-ILs-C8-LaW₁₀; FT-IR spectra (b), solid-state ²⁹Si CP/MAS NMR spectra (c) and XPS spectra for the W4f core level (d) of the fresh and used Mg₃Al-ILs-C8-LaW₁₀.

It is essential to investigate the activity and stability of the catalyst for epoxidation of allylic alcohols for practical application. Taking the *trans*-2-hexen-1-ol as an example, the recycling experiments have been performed using Mg₃Al-ILs-C8-LaW₁₀. The solid catalyst can be readily separated from the reaction mixture by centrifugation and the recycling experiments have been carried out five times by re-addition substrates and H₂O₂ (30 wt. %) at 25 °C (Figure 6a). There is no obvious loss of the initial catalytic activity (the conversion for fresh catalyst: 96.0 %; 1st: 93.2; 2nd: 94.7, 3rd: 93.0 %; 4th: 92.4; 5th: 92.1 %) and the selectivity remains 99 %. No leaching of tungsten into the reaction system was detected by inductively coupled plasma atomic emission analysis (ICP-AES).

FT-IR spectra of the fresh and reused catalyst Mg₃Al-ILs-C8-LaW₁₀ exhibit nearly same peaks at 1658; 936, 840 and 778 cm⁻¹ (Figure 6b), which could be assigned to the C=N stretching vibrations of ILs and the vibration associated with the LaW₁₀ cluster, respectively. Compared the solid-state ²⁹Si crosspolarization magic-angle spinning (CP/MAS) NMR spectra of the fresh and recycled Mg₃Al-ILs-C8-LaW₁₀, they both exhibit the resonance at -66.7 ppm (Figure 6c). Moreover, the oxidation state of W in fresh and recycled Mg₃Al-ILs-C8-LaW₁₀ is +6, indicating

the good stability of the LaW10 active centers (Figure 6d). These results reveal that the structure of the recycling catalyst Mg3Al-ILs-C8-LaW10 retained its structural integrity, composition and performance during the series of consecutive catalytic cycles.

We propose a possible catalytic mechanism for the current epoxidation (Figure S9).[2,4,44] Firstly, the catalytic active species of peroxotungstate are generated by LaW10 located in the restricted region of LDHs in the presence of H₂O₂; Secondly, the -H bond in the allylic alcohols could get access to the active species by ligating to tungstate atom to form a tungstenalcoholate species; Subsequently, the deprotonation of the O-H bond of an allylic alcohol is accompanied by a proton transfer to the peroxy ligand; Further on, the peroxide part forms an electronegative conjugated system followed by a double bond formation generating an intermediate state (step 3); Finally, the epoxides are formed, leading to the original structure of W coordination (step 4).

Conclusion

In summary, the POM anion of LaW10 has been successfully intercalated into the ionic liquids (ILs) modified LDHs for the first time, leading to the formation of the Mg₃Al-ILs-C_n-LaW10 (n = 4, 8, 12) employing an exfoliation and assembly synthetic approach. The resulting intercalation catalysts have been fully characterized by various techniques. Epoxidation of various allylic alcohol to the corresponding epoxides using Mg₃Al-ILs-C₈-LaW10 as heterogeneous catalyst was demonstrated in the presence of H₂O₂ under mild and solvent-free conditions with an excellent conversion and selectivity. Additionally, this catalytic system exhibits remarkable catalytic efficiency for the epoxidation of long chain hydrophobic allylic alcohols as well. For example, the Mg₃Al-ILs-C₈-LaW10 composite material catalyzed the epoxidation of *trans*-2-hexen-1-ol, with 96 % conversion and 99 % epoxide selectivity at 25 °C in 2.5 h under solvent-free condition. Furthermore, the catalyst can be separated easily and recycled for more than 5 times without obvious loss of catalytic activity. The structural integrity as well as the composition of the intercalation catalyst Mg₃Al-ILs-C₈-LaW10 remains unaltered during the course of the catalytic reactions. Therefore, the cooperative effect between LaW10, LDHs and ILs offers a highly effective, green epoxidation system. The prepared heterogeneous catalyst shows a great potential for further application.

Experimental

Chemicals and Materials: All chemicals were of analytical grade and were used as received without any further purification. The 2-buten-1-ol, 3-methyl-2-buten-1-ol, *cis*-2-penten-1-ol, *trans*-2-hexen-1-ol, *cis*-2-hexen-1-ol, *trans*-2-hepten-1-ol, *trans*-2-octen-1-ol, geraniol, *cis*-2-nonen-1-ol, *trans*-2-nonen-1-ol, hexamethylenetetramine, Na₂WO₄·2H₂O, CH₃CN, CHCl₃, CH₃CH₂OH, LaCl₃·7H₂O were purchased from Alfa Aesar, NaOH, Mg(NO₃)₂·6H₂O, Al(NO₃)₃·9H₂O, HNO₃, NH₃·H₂O, H₂O₂, acetic acid, were purchased from Beijing Chemical Company. The Na₉LaW₁₀O₃₆·32H₂O (LaW10),[45] [Mg_{0.75}Al_{0.25}(OH)₂](CO₃)_{0.125}·2H₂O (Mg₃Al-CO₃),[46] [Mg_{0.75}Al_{0.25}(OH)₂](NO₃)_{0.25}·2H₂O (Mg₃Al-NO₃),[47] 1-butyl-3-(3-triethoxysilylpropyl)-4,5-dihydroimidazolium hexafluorophosphate (EtO)₃Si-ILs-C4), 1-octyl-3-(3-triethoxysilylpropyl)-4,5-dihydroimidazolium hexafluorophosphate (EtO)₃Si-ILs-C8), 1-dodecyl-3-(3-triethoxysilylpropyl)-4,5-dihydroimidazolium hexafluorophosphate (EtO)₃Si-ILs-C12),[48] were synthesized and characterized according to the literature procedure.

Instruments: Fourier transform infrared (FT-IR) spectra were recorded on a Bruker Vector 22 infrared spectrometer by using KBr pellet method. The solid-state NMR experiments were carried out on a Bruker Avance 300M solid-state spectrometer equipped with a commercial 5 mm MAS NMR probe. Thermogravimetric (TG) analysis was done on STA-449C Jupiter (HCT-2 Corporation, China) with a heating rate of 10 °C min⁻¹ from 25 to 800 °C in flowing N₂ (20 mL/min). BET measurements were performed at 77 K on a Quantachrome Autosorb-1C analyzer. N₂ adsorption-desorption isotherms were measured using Quantachrome Autosorb-1 system at liquid nitrogen temperature. Inductively coupled plasma-atomic emission spectroscopy (ICP-AES) analysis was performed on a Shimadzu ICPS-7500 instrument. X-ray photoelectron spectroscopy (XPS) measurements were performed with monochromatized Al K exciting X-radiation (PHI Quantera XM). Scanning electron microscopy (SEM) images and energy dispersive X-ray spectroscopy (EDS) analytical data were obtained using a Zeiss Supra 55 SEM equipped with an EDS detector. The powder X-ray diffraction (XRD) analysis was carried out on a Bruker D8 diffractometer with high-intensity Cu-K α radiation ($\lambda = 0.154$ nm). High resolution Transmission Electron Microscopy (HRTEM) was conducted on JEOL JEM-2100 under an accelerating voltage of 400 kV. N₂ adsorption/desorption isotherms were measured using a Quantachrome Autosorb-1 system at liquid-

nitrogen temperature. ¹H-NMR and ¹³C-NMR spectra were recorded on a Bruker AV400 NMR spectrometer at resonance frequency of 400 MHz, and the chemical shifts were given relative to TMS as the internal reference. The products of the catalytic reactions of allylic alcohols were analysed by Agilent 7820A gas chromatography (GC) system using a 30 m 5 % phenylmethyl silicone capillary column with an ID of 0.32 mm and 0.25 μm coating (HP-5). The products were identified using reference standards.

Synthesis of Mg₃Al-ILs-Cn-LaW₁₀ (n=4, 8, 12): Mg₃Al-NO₃ (0.5 g) was added into 500 mL of formamide in a three-necked flask, which was purged with N₂ to avoid carbonate contamination. The mixture was vigorously stirred for 2 days. After that, the mixture was centrifuged for 10 min and the suspension was separated simply by filtration. Then, (EtO)₃Si-ILs-Cn (4.4 mmol, n=4, 8, 12) was dissolved in CH₃CN/CH₂Cl₂ (1:1, 5 mL) and added dropwise to the above isolated suspension. After that, the reaction mixture was kept for stirring under N₂ for 24 hours. The LaW₁₀ (1.85 g) was dissolved in 50 mL formamide and added dropwise to the above solution. The resultant precipitate of Mg₃Al-ILs-Cn-LaW₁₀ (~1.0 g) was collected by filtration and washed with ethanol and water, and dried under vacuum overnight.

Catalytic test: In a typical experiment, a mixture of 2 mmol *trans*-2-hexen-1-ol, 2.4 mmol H₂O₂ (30 wt. %), and 20 mg catalyst (3.88 μmol based on LaW₁₀) were added into a 10 mL glass bottle at 25 °C and the reaction mixture was kept for stirring vigorously. The reaction was effectively quenched by adding diethyl ether (6 mL) and H₂O (1.5 mL) after 2.5 hours. The resulting products were extracted by diethyl ether, analyzed by GC and identified by ¹H-NMR and ¹³C-NMR to determine the conversion and selectivity.

Acknowledgements

This research was supported by the National Basic Research Program of China (973 program, 2014CB932104), National Science Foundation of China (U1407127, U1507102), Fundamental Research Funds for the Central Universities (YS1406), China Postdoctoral Science Foundation (2014M560878).

Reference

- [1] C. Chen, H. Y. Yuan, H. F. Wang, Y. F. Yao, W. B. Ma, J. Z. Chen, Z. S. Hou, *ACS. Catal.* **2016**, 6, 3354-3364.
- [2] K. Kamata, K. Yamaguchi, N. Mizuno, *Chem. Eur. J.* **2004**, 10, 4728- 4734.
- [3] K. A. Jørgensen, *Chem. Rev.* **1989**, 89, 431-458.
- [4] W. Adam, T. Wirth, *Acc. Chem. Res.* **1999**, 32, 703-710.
- [5] S. A. Hauser, M. Cokoja, F. E. Kühn, *Catal. Sci. Technol.* **2013**, 3, 552- 561.
- [6] a) S. S. Wang, G. Y. Yang, *Chem. Rev.* **2015**, 115, 4893-4962; b) W. Dai, G. S. Li, B. Chen, L. Y. Wang, S. Gao, *Org. Lett.* **2015**, 17, 904-907.
- [7] F. G. Gelalcha, B. Bitterlich, G. Anilkumar, M. K. Tse, M. Beller, *Angew. Chem. Int. Ed.* **2007**, 46, 7293-7296.
- [8] Y. Nishikawa, H. Yamamoto, *J. Am. Chem. Soc.* **2011**, 133, 8432-8435.
- [9] W. Adam, P. L. Alsters, R. Neumann, C. R. Saha-Möller, D. Sloboda- Rozner, R. Zhang, *J. Org. Chem.* **2003**, 68, 1721-1728.
- [10] K. Kamata, K. Sugahara, K. Yonehara, R. Ishimoto, N. Mizuno, *Chem. Eur. J.* **2011**, 17, 7549-7559.
- [11] T. A. G. Duarte, I. C. M. S. Santos, M. M. Q. Simões, M. G. P. M. S. Neves, A. M. V. Cavaleiro, J. A. S. Cavaleiro, *Catal. Lett.* **2014**, 144, 104-111.
- [12] N. Mizuno, K. Yamaguchi, K. Kamatab, *Coord Chem Rev.* **2005**, 249, 1944-1956.
- [13] S. Abednatanzi, A. Abbasi, M. Masteri-Farahani, *J. Mol. Catal. A-Chem.* **2015**, 399, 10-17.
- [14] M. Noji, T. Kobayashi, Y. Uechi, A. Kikuchi, H. Kondo, S. Sugiyama, K. Ishii, *J. Org. Chem.* **2015**, 80, 3203-3210.
- [15] S. Bhunia, S. Jana, D. Saha, B. Dutta, S. Koner, *Catal. Sci. Technol.* **2014**, 4, 1820-1828.
- [16] M. S. Saraiva, C. D. Nunes, T. G. Nunes, M. J. Calhorda, *Appl. Catal. A-Gen.* **2013**, 455, 172-182.
- [17] C. I. Fernandes, M. D. Carvalho, L. P. Ferreira, C. D. Nunes, P. D. Vaz, *J. Organomet. Chem.* **2014**, 760, 2-10.
- [18] K. Kamata, T. Hirano, S. Kuzuya, N. Mizuno, *J. Am. Chem. Soc.* **2009**, 131, 6997-7004.
- [19] T. L. Greaves, C. J. Drummond, *Chem. Rev.* **2015**, 115, 11379-11448.
- [20] a) S. Herrmann, M. Kostrzewa, A. Wierschem, C. Streb, *Angew. Chem. Int. Ed.* **2014**, 53,

- 13596-13599; b) J. Li, D. F. Li, J. Y. Xie, Y. Q. Liu, Z. J. Guo, Q. Wang, Y. N. Lyu, Y. Zhou, *J. Catal.* **2016**, 339, 123-134.
- [21] Y. Leng, J. W. Zhao, P. P. Jiang, J. Wang, *ACS. Appl. Mater. Inter.* 2014, 6, 5947-5954.
- [22] H. Sven, S. Andrey, S. Carsten, *J. Molec. Engin. Mater.* **2014**, 2 1440001-1440007.
- [23] G. L. Fan, F. Li, D. G. Evans, X. Duan, *Chem. Soc. Rev.* **2014**, 43, 7040-7066.
- [24] S. Omwoma, W. Chen, R. Tsunashima, Y. F. Song, *Coordin. Chem Rev.* **2014**, 58-71, 258-259.
- [25] Y. Q. Jia, Y. J. Fang, Y. K. Zhang, H. N. Miras, Y. F. Song, *Chem. Eur. J.* **2015**, 21, 14862 – 14870.
- [26] Y. Chen, Z. X. Yao, H. N. Miras, Y. F. Song, *Chem. Eur. J.* **2015**, 21, 10812-10820.
- [27] M. V. Reddy, N. T. K. Lien, G. C. S. Reddy, K. T. Lim, Y. T. Jeong, *Green Chem.* **2016**, 18, 4228-4239.
- [28] G. L. Huang, S. L. Ma, X. H. Zhao, X. J. Yang, K. Ooi, *Chem. Mater.* **2010**, 22, 1870-1877.
- [29] A. Y. Park, H. Kwon, A. J. Woo, S. J. Kim, *Adv. Mater.* **2005**, 17, 106-109.
- [30] S. Zhao, J. H. Xu, M. Wei, Y. F. Song, *Green Chem.* **2011**, 13, 384-389.
- [31] R. D. Peacock, T. J. R. Weakley, *J. Chem. Soc. A.* **1971**, 1836-1839.
- [32] L. Salvati, L. E. Makovsky, J. M. Stencel, F. R. Brown, D. M. Hercules, *J. Phys. Chem.* **1981**, 85, 3700-3707.
- [33] D. V. Deubel, G. Frenking, P. Gisdakis, W. A. Herrmann, N. Rösch, J. Sundermeyer, *Acc. Chem. Res.* **2004**, 37, 645-652.
- [34] P. Liu, H. Wang, Z. C. Feng, P. L. Ying, C. Li, *J. Catal.* **2008**, 256, 345-348.
- [35] F. Farzaneh, Y. Sadeghi, *J. Mol. Catal. A-Chem.* **2015**, 398, 275-281.
- [36] W. Chuan, Y. Hisashi, *J. Am. Chem. Soc.* **2014**, 136, 1222-1225.
- [37] R. Mello, A. Alcalde-Aragones, M. E. G. Nunez, G. Asensio, *J. Org. Chem.* **2012**, 77, 6409-6413.
- [38] S. Doherty, J. G. Knight, J. R. Ellison, D. Weekes, R. W. Harrington, C. Hardacre, H. Manyar, *Green Chem.* **2012**, 14, 925-929.
- [39] C. I. Fernandes, M. S. Saraiva, T. G Nunes, P. D. Vaz, C. D. Nunes, *J. Catal.* **2014**, 309, 21-32.
- [40] M. V. Vasylyev, R. Neumann, *J. Am. Chem. Soc.* **2004**, 126, 884-890.
- [41] N. Mizuno, K. Yamaguchi, *Chemical Record*, **2006**, 6, 12-22.
- [42] P. Liu, C. H. Wang, C. Li, *J. Catal.* **2009**, 262, 159-168.

- [43] C. Chen, X. G. Zhao, J. Z. Chen, L. Hua, R. Zhang, L. Guo, B. N. Song, H. M. Gan, Z. S. Hou, *Chemcatchem*. **2014**, 6, 3231-3238.
- [44] W. Adam, C. M. Mitchell, C. R. Saha-Möller, *J. Org. Chem.* **1999**, 64, 3699-3707
- [45] J. H. Xu, S. Zhao, Y. C. Ji, Y. F. Song, *Chem. Eur. J.* **2013**, 19, 709-715.
- [46] N. Iyi, Y. Ebina, T. Sasaki, *J. Mater. Chem.* **2011**, 21, 8085-8095.
- [47] Y. Q. Jia, S. Zhao, Y. F. Song, *Appl. Catal. A-Gen.* **2014**, 487, 172-180.
- [48] Y. Chen, Y. F. Song, *ChemPlusChem.* 79, **2014**, 304-309.